physica status solidi c
www.pss-c.com
current topics in solid state physics

Spectroscopic ellipsometry of materials for infrared micro-device fabrication

W. R. Folks, J. Ginn, D. Shelton, J. Tharp, and G. Boreman

College of Optics & Photonics, CREOL & FPCE, University of Central Florida, Orlando, Florida, 32816-2700, USA

Received 7 June 2007, revised 30 October 2007, accepted 20 November 2007
Published online 22 February 2008

PACS 78.20.Ci, 78.30.Hv, 78.30.Jw, 85.60.-q

For many common types of process materials used in the fabrication of infrared microelectronic devices there is a lack of information available in the literature regarding their thin-film optical properties over the wavelength range of 2 to 30 micrometers. In this article, spectroscopic ellipsometry is used to determine room-temperature optical constants in the infrared for a variety of organic and inorganic coatings commonly used in fabrication. Examples include coatings used for photolithography, coating, passivation, planarization, index matching, and stand-off. Applications include infrared frequency selective surfaces, antennas, micro-displays, and flexible substrates.

phys. stat. sol. (c) **5**, No. 5, 1113–1116 (2008) / **DOI** 10.1002/pssc.200777748

WILEY-VCH

phys. stat. sol. (c) **5**, No. 5, 1113–1116 (2008) / **DOI** 10.1002/pssc.200777748

physica status solidi c
www.pss-c.com
current topics in solid state physics

Spectroscopic ellipsometry of materials for infrared micro-device fabrication

W. R. Folks[*], J. Ginn[**], D. Shelton, J. Tharp, and G. Boreman

College of Optics & Photonics, CREOL & FPCE, University of Central Florida, Orlando, Florida, 32816-2700, USA

Received 7 June 2007, revised 30 October 2007, accepted 20 November 2007
Published online 22 February 2008

PACS 78.20.Ci, 78.30.Hv, 78.30.Jw, 85.60.-q

[*] Corresponding author: e-mail wfolks@mail.ucf.edu, Phone: +1 407 823 6904, Fax: +1 407 823 6880
[**] e-mail jcginn@mail.ucf.edu, Phone: +1 407 823 6922

For many common types of process materials used in the fabrication of infrared microelectronic devices there is a lack of information available in the literature regarding their thin-film optical properties over the wavelength range of 2 to 30 micrometers. In this article, spectroscopic ellipsometry is used to determine room-temperature optical constants in the infrared for a variety of organic and inorganic coatings commonly used in fabrication. Examples include coatings used for photolithography, coating, passivation, planarization, index matching, and stand-off. Applications include infrared frequency selective surfaces, antennas, micro-displays, and flexible substrates.

1 Introduction In this article infrared reflective ellipsometry (*refl*-SE) [1, 2] is used to determine room temperature optical constants in the infrared for a variety of common materials used in micro-electronic device fabrication. There are many excellent texts which review the fundamentals of the technique [3, 4]. Materials studied include polymers such as polyimide, BCB (a benzocyclobutene-based polymer), and FOx (flowable oxide); resists such as PMMA (polymethyl methacrylate), PMGI (polydimethylglutarimide), SU-8, ZEP; inorganic insulators such as ZrO_2 (zirconium dioxide, sometimes called zirconia), Si_3N_4 (silicon nitride), and vanadium oxide (VO_x). The optical properties of these materials have been studied many times. However, there exist gaps in the available literature for the optical constants of these materials in the infrared part of the electromagnetic spectrum.

BCB is a spin-on polymer based on benzo-cyclobutene developed by the Dow Chemical Co. used as a dielectric insulator for electronic packaging and display technology [3]. For infrared microelectronic devices, BCB is highly desirable for its ease of deposition and solvent resistance. The specific version of BCB considered in this paper is product code 3022-35 of Dow's Cyclotene^{TM} 3000 series. Polyimide, manufactured by DuPont Corp. and also known also under the brand name Kapton®, is a polymer of imides and may be obtained in sheet form or as a resin which may be dissolved in a solvent and spin coated onto a substrate. Polyimide has applications in the electronics industry and for liquid crystal displays where it is used as a molecular alignment layer. This alignment layer is important because it controls surface anchoring energy and pretilt angle of the liquid crystal molecules pinned at the substrate as well as their orientation. Polyimide is also commonly used in the fabrication of flexible or conformal structures. Kapton® has been shown to be anisotropic due to stretching during manufacture and exhibits dichroism at 1355 cm^{-1} due to the C-N-C bond [6, 7]. In this paper polyimide was studied without post-bake processing to retain a homogeneous layer and avoid the complexities of an anisotropic sample. The flowable oxide FOx-16 from Dow Chemical Co. is an inorganic polymer based on hydrogen silsesquioxane which can be spin coated onto a substrate [8]. It is an ideal material for planarization.

Knowing the IR optical constants of resists is important for some applications where photoresist layers may be left as insulating layers or structural supports. Resists have been studied for applications involving two-photo absorption techniques in lithographically prepared 3-D networks [9]. PMMA is acrylic, and its structure is well known [10]. PMGI, developed by Microchem, is often used as an undercutting layer for other high resolution resists to aide deposition. SU-8, also developed by Microchem, is a viscous negative resist commonly used for MEMS, micromachining, and optical mask manufacturing [11–13]. ZEP

is a positive tone, high resolution e-beam resist developed by Zeon Corporation that has recently become popular for e-beam lithography. SU-8 and ZEP [14] may be used for high resolution EUV or X-ray lithography.

Finally, in Section 3.1 we study vanadium pentoxide (V_2O_5) which is a common bolometric material or xerogel [15]. Silicon nitride and zirconia (a hard ceramic), are often used as isolation or stand-off layers in microdevice fabrication in place of organic materials higher standards for vibration, mechanical shock, and thermal requirements [16].

2 Experimental Our laboratory is equipped with an automated high resolution infrared ellipsometer with a wavelength range from 2 to 30 μm, suited for either thin film or bulk characterization. The instrument uses the rotating compensator method of ellipsometry to measure intensity and phase (Ψ and Δ) information, and can measure Ψ from 0 to 90°, and the advantage of being able to measure Δ from 0 to 360° [3, 4]. The source is a Fourier-transform infrared (FTIR) spectrometer of up to 1 cm^{-1} resolution. The detector may be positioned anywhere from 25° to 90°. Measurements are typically done at 8 cm^{-1} resolution or less. Multiple scans are performed near the Brewster angle at different detector angles to increase resolution. To minimize depolarization of the signal the back of the sample is roughened and a matte finish adhesive applied to scatter light reflected off the back surface. In some cases the film to be tested is deposited directly on to a well characterized, highly reflective metal to simplify modelling.

The resulting Ψ and Δ data is fit to a model consisting of a linear superposition of Gaussian or Lorentzian oscillator functions, Σ f_i. Each term in the series is Kramers-Kronig consistent and represents a mode of oscillation of the molecule and a corresponding absorption peak. The modelling software can account for non-idealities such as thickness nonuniformity, signal depolarization, source bandwidth, and angular spread [17]. It can also model surface roughness and interfacial zones as well as determine anisotropy and surface roughness characteristics.

From the *refl*-SE data, Ψ and Δ are then fit simultaneously for multiple detector angles to the general equation of ellipsometry, $\rho = \tan\Psi e^{i\Delta}$. Where $\tan\Psi = |R_P|/|R_S|$ for the *S* and *P* polarizations, and $\Delta = \delta_1 - \delta_2$ is the phase shift upon reflection from the sample. From this result, values of *n* and κ for the complex index of refraction ($\tilde{n} = n + i\kappa$), or ε_1 and ε_2 for the complex permittivity ($\tilde{\varepsilon} = \varepsilon_1 + i\varepsilon_2$) may be determined as well as film thickness. The absorption coefficient α is determined by the relation $\alpha = 4\pi\kappa/\lambda$.

3 Results and discussion

3.1 Spin-on polymers All of the polymers samples were prepared by spin coating or e-beam evaporation onto a silicon wafer or gold film according to manufacturer's specifications. Typical film thicknesses range from 100 nanometers to 1 micron. Note that in some figures we have reduced the number of points plotted to prevent crowding and improve readability. This does not indicate the resolution of our instrument but serve only as a guide for the eye. Resolution is 8 cm^{-1} unless otherwise stated.

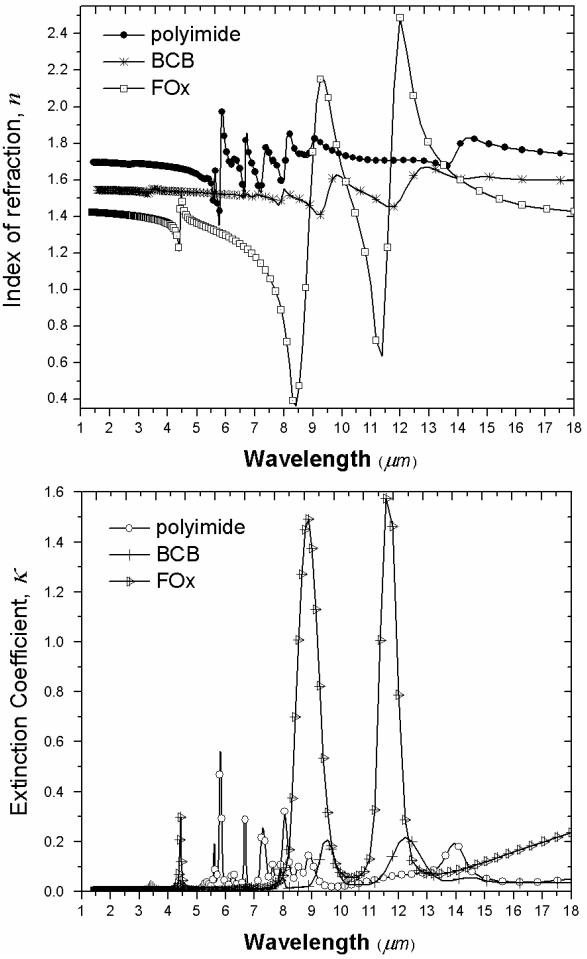

Figure 1 Optical constants for polyimide PI-2525, BCB, and FOx-16. Film thicknesses: 1531 nm, 1439 nm, 116 nm respectively.

Figure 1 shows the optical constants for polyimide, BCB, and FOx. In the near-IR all three materials have nearly constant *n* and κ values out to about 4 μm except for a weak feature which represents the common asymmetric and symmetric C-H stretch modes at 2920 cm^{-1} (3.43 μm) and 2853 cm^{-1} (3.51 μm) for polyimide and BCB [18]. The same features are observed in Fig. 2 for the resists. Although not unexpected, it is of interest to point out that the spectral content of the polyimide specimen is quite complex in comparison with the other two materials, requiring 18 Gaussian oscillators to model the data. In addition, due to the C-H stretch modes we also observe the common methylene scissoring and umbrella modes for polyimide at

1466 cm^{-1} (6.83 μm) and 1377 cm^{-1} (7.26 μm) respectively are observed. These peaks are seen in the spectrum of SU8 and ZEP as well. Bands which may be attributed to the imine rings of polyimide are observed at 1775, 1720, and 705 cm^{-1} (5.63, 5.81, and 14.18 μm) [7, 19], while the feature at 830 cm^{-1} is due to an ether moiety [20]. In addition, polyimide possesses weaker absorption lines from 5 to 7 μm most likely due to vibrations of the benzene ring, and from 7 to 10 μm due to C-H deformation modes [21].

The spectral structure of BCB is less complex compared to polyimide or FOx. Absorption peaks due to the Si-CH_3 bond is identified at 1250 cm^{-1} (8.0 μm) and the Si-O-Si bond at 1049 cm^{-1} (9.53 μm) [5], as well as the previously mentioned asymmetric and symmetric C-H stretch modes at 2920 cm^{-1} and 2853 cm^{-1}.

FOx is perhaps the most interesting of the three sets of curves. FOx is dominated by two large absorption peaks at 9 and 11.5 μm and a smaller peak at 4.5 μm. The dominant features of FOx-16 are the Si-O stretch at 1125 cm^{-1} (8.89 μm), and the Si-O bend modes at 861cm^{-1} and 830 cm^{-1} where the two peaks are barely resolvable in Fig. 1 (11.61 μm and 12.05 μm respectively) [22]. The weaker Si-H stretch is seen at 2260 cm^{-1} (4.42 μm).

Note that for both BCB and polyimide the range over which n and k vary from mid- to long-wave IR bands is small compared to FOx. BCB has an index of refraction which consistently remains slightly below the polyimide curve, and both curves are relatively transparent over most of the wavelength range of the figure. On the other hand, FOx is superior, in terms of lower index, to both BCB and polyimide in the NIR and will provide a better match to SiO_2 in this spectral range. Beyond 18 μm (not shown) all three curves show normal dispersion with no significant absorption peaks within the range of the instrument.

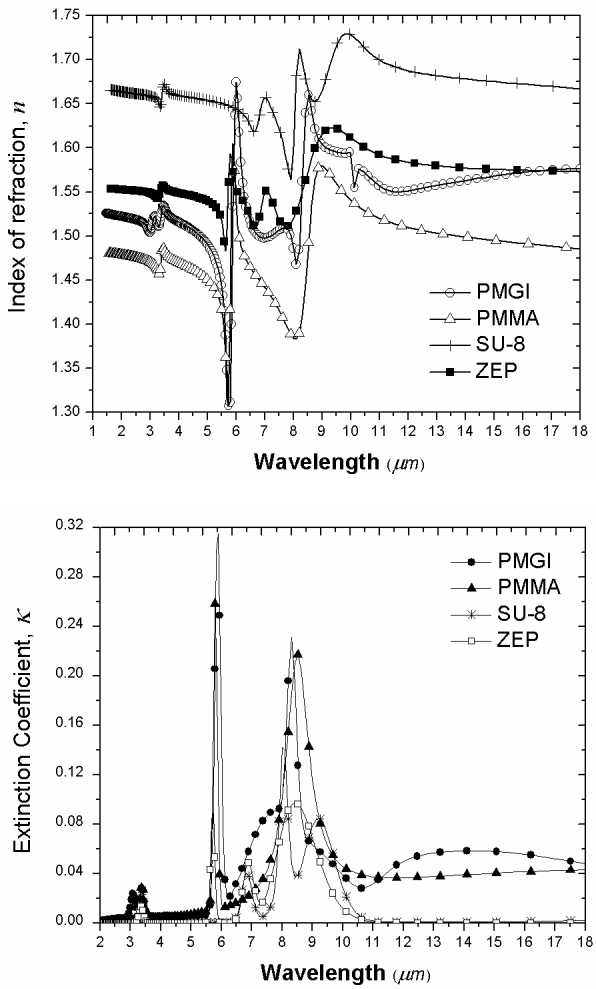

Figure 2 Optical constants for PMGI, PMMA, SU-8, and ZEP-520. Film thicknesses: 1875 nm, 303 nm, 1817 nm, 285 nm respectively.

3.2 Lithographic resists Figure 2 presents the measured optical constants for several resists under study. Predictably, all of the resists demonstrate similar spectral behavior. A strong, narrow absorption peak exists for PMMA and PMGI around 6.1 μm due to the imide group, and another broader peak in the 8-12 μm LWIR band around 8.4 μm, possibly a C-C-O stretching mode, except that SU-8 is resolved into a double peak around 8.4 μm with maxima at 8.0 and 9.2 μm. All four resists also have a small feature around 3.4 μm (PMGI has an additional peak at 3.1 μm). Beyond the long wave infrared band (LWIR) all four resists begin to exhibit normal dispersion. The absorption peaks for the resists are all significantly weaker than the dominant peaks of FOx in Fig. 1 or materials shown in Fig. 3.

3.3 Inorganic insulators Figure 3 contains the optical constants for Si_3N_4, ZrO_2, and V_2O_5. The scale ranges from 2 to 30 μm to show the behavior beyond the LWIR band where notable features are still present, unlike the polymers. Both ZrO_2 and V_2O_5 have small features near 3 μm and ZrO_2 has a shoulder at 3.5 μm and a small double peak at 6.4 and 7.0 μm. The n and k curves for ZrO_2 increase at longer wavelengths with a shoulder around 16 μm and large peak at 23.3 μm. The principle feature of V_2O_5 is the double peak at 13.0 and 16.2 μm. Si_3N_4 is dominated by a large Si-N absorption band [23] at 11.2 μm (893 cm^{-1}) with a shoulder at 8.70 μm (1150 cm^{-1}), limiting its applications for use with the 10.6 μm line CO_2 laser. The narrow Si-O peak expected at 1100 cm^{-1} is not resolved by the model [23].

The index of refraction for Si_3N_4 and V_2O_5 changes rapidly with wavelength in the 8-12 μm LWIR which would cause dispersion issues for a broad band LWIR optical design.

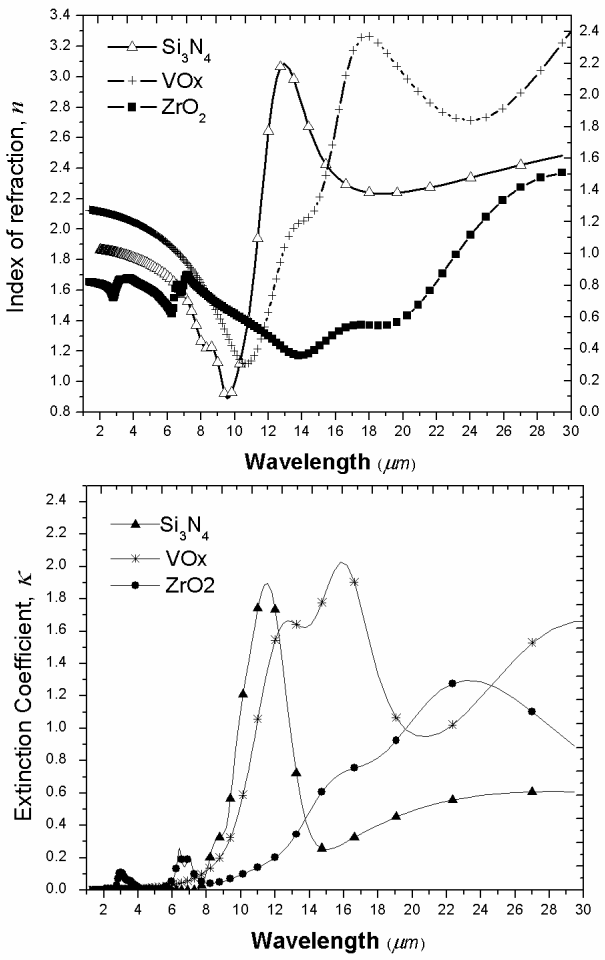

Figure 3 Optical constants for PECVD silicon nitride, vanadium pentoxide, and zirconium dioxide. Film thicknesses: 207 nm, 192 nm, 455 nm respectively.

4 Conclusion In this paper we have presented optical constants in the infrared for a number of common materials used in micro-device fabrication from reflective spectroscopic ellipsometry measurements. The spectra presented agree well with theory and the data collected will aid in filling the gaps of prior studies. Additional discussion has been presented for potential operating ranges and applications of each material.

Acknowledgements We wish to thank Mr. Greg Pribil of J. A. Woollam Corporation, and Mr. Corey Bungay of Lockheed Martin Corporation for many useful discussions.

References

[1] M. Schubert, C. Bundesmann, H. v. Weckstern, G. Jakopic, A. Haase, N.-K. Persson, F. Zhang, H. Arwin, and O. Inganäs, Appl. Phys. Lett. **84**, 1311-1313 (2004).
[2] W. Folks, S. Pandey, G. Pribil, D. Slafer, M. Manning, and G. Boreman, Intl J. Infrared Millim. Waves **27**, 1553-1571 (2006).
[3] H. G. Tompkins, Handbook of Ellipsometry (William Andrew Inc., New York, 2005).
[4] H. Fujiwara, Spectroscopic Ellipsometry: Principles and Applications (Wiley, New York, 2007).
[5] J. T. Beechinor, E. McGlynn, M. O'Reilly, and G. M. Crean, Microelectron. Eng. **33**, 363-368 (1997).
[6] C. Bungay and T. Tiwald, Thin Solid Films **455/456**, 272-277 (2004).
[7] M. M. Ellison and L. T. Taylor, Chem. Mater. **6**, 990-998 (1994).
[8] F. Salmassi, P. Naulleau, and E. M. Gullikson, Appl. Opt. **45**, 2404-2408 (2006).
[9] S. Kuebler and M. Rumi, in: Encyclopedia of Modern Optics, edited by R. D. Guenther, D. G. Steel, and L. Bayvel (Elsevier, Oxford, 2004), pp. 189-206.
[10] J. Licari and L. Hughes, Handbook of Polymer Coatings for Electronics - Chemistry, Technology and Applications (William Andrew Publishing, 1990).
[11] A. L. Bogdanov and S. S. Peredkov, Microelectron. Eng. **53**, 493-6 (2000).
[12] V. Seidemann, J. Rabe, M. Feldmann, and S. Büttgenbach, Micro. Syst. Tech. **8**, 348-350 (2002).
[13] M. C. Peterman, P. Huie, D. M. Bloom, and H. A. Fishman, J. Micromech. Microeng. **13**, 380-382 (2003).
[14] W. Chen, Y. Morikawa, M. Itoh, T. Hayashi, K. Sugita, H. Shindo, and T. Uchida, J. Vac. Sci. Technol. A **17**, 2546-2550 (1999).
[15] F. Gonzalez, M. Abdel-Rahman, and G. Boreman, Microwave Opt. Tech. Lett. **38**(3), 235-237 (2003).
[16] C. Middleton and G. Boreman, J. Vac. Sci. Tech. B **24**(5), 2356-2359 (2006).
[17] WVASE32 software (J.A. Woollam Co., Inc., Lincoln, NE, USA).
[18] A. J. Luff, DMS Working Atlas of Infrared Spectroscopy, (Butterworths, London, 1972).
[19] M. Navarre and K. L. Mittal (Ed.), Polyimides: Synthesis, Characterization, and Applications (Plenum Press, New York, 1984), pp. 438-439.
[20] R. M. Silversein, G. C. Bassler, and T. C. Morrill (Eds.), Spectrometric Identification of Organic Compounds, 4th ed. (Wiley, New York, 1981), pp. 116, 133.
[21] D. Dolphin and A. Wick, Tabulation of Infrared Spectral Data (Wiley, New York, 1977), chap. 1.
[22] Flowable Oxide Technical Brief (Dow Corning, Corp., Midland, MI, USA, 2005).
[23] F. Rasmussen, in: Proceedings of Internat. Symp. Dielectrics in Emerging Technologies, Paris, France, 2003, pp. 218-229.

